Quantum Electronics **40** (2) 121 – 126 (2010)

PACS numbers: 42.65.Jx; 42.65.Re; 33.80.Eh; 52.50.Jm
DOI: 10.1070/QE2010v040n02ABEH014199

Filamentation of high-power laser radiation in air and water: Comparative analysis

Yu.E. Geints, A.A. Zemlyanov

***Abstract*. The propagation of high-power femtosecond laser pulses is considered in the self-focusing and filamentation formation regime. Similarities and differences in the character of the laser beam filamentation are analysed qualitatively and quantitatively in the atmospheric air and water. Based on the numerical results, the most important parameters (radius, intensity, free electron density) in light and plasma filaments produced by ultrashort laser pulses are shown to depend strongly on the optical parameters of the propagation medium, and, first of all, on the Kerr nonlinearity coefficients and the photoionisation rate of the medium molecules.**

Keywords: *femtosecond laser radiation, beam filamentation, nonstationary self-focusing of pulsed laser radiation, medium photoionisation.*

1. Introduction

The propagation of ultrashort high-power laser radiation in gas and condensed media is accompanied by its filamentation and considerable changes in the energy, spatial, spectral, and angular parameters. The state of the art of this problem is presented in detail in reviews [1 – 4].

The physical reason behind the filamentation effect is the cubic nonlinearity of the medium refractive index, which causes the self-focusing of a light wave, thereby leading, during the propagation of light pulses, to their progressive compression over the spatial coordinates. Radiation diffraction and some physical mechanisms, among which plasma formation dominates in gases and condensed media, counteract the developing spatial pulse compression. The medium photoionisation causes nonlinear energy losses in the radiation channel and stops the further growth of its intensity in the filament region.

Filamentation of ultrashort laser pulses leads to significant changes in their frequency spectrum. Due to the self-phase modulation of the light wave, radiation with an anomalously broad spectrum – supercontinuum – is produced. The spectral width of this radiation substantially exceeds the initial width and, as a rule, covers the UV and near-IR regions. This spectral broadening is mainly caused by the Kerr and plasma nonlinearities of a medium.

The angular spectrum of ultrashort pulses also experiences drastic changes during the nonlinear propagation of the pulse in the medium. The initial spatial profile of the laser beam broadens during self-focusing and, thus, acquires a number of new intense angular components to which, in the beam cross section, rings surrounding the higher-intensity regions correspond.

It is important to emphasize that despite serious differences in the physical and optical properties of media in which filamentation of ultrashort laser pulses (condensed, gaseous) is observed experimentally, the above-described scenario of the process is on the whole universal. The peculiarity of each medium is manifested in the characteristic scales of the nonlinear radiation conversion and in specific values of the filamentation parameters in the beam. It is obvious that in the practical research in the field of femtosecond atmospheric optics, it is very important to have a clear idea of how the physical properties of the laser beam propagation medium will affect the quantitative characteristics of the beam filamentation. Despite the impressive number of presently available scientific papers on the femtosecond subject, we have failed to find a single-minded analysis of similarities and differences in the laser beam filamentation in physically different media.

In this paper, based on the numerical calculations performed within the framework of the conventional model of the nonstationary self-focusing of high-power ultrashort pulses, we have performed a comparative analysis of the filamentation properties of femtosecond laser pulses in two most widespread natural media – atmospheric air and water. We pay the main attention to comparison of scale, energy, and spectral characteristics of light and plasma filaments produced in the beam channel during the propagation of radiation in the media under study.

2. Theoretical model of ultrashort pulse self-focusing

As a mathematical basis for simulating the propagation of ultrashort pulses in a transparent medium, we will use the formalism of the nonlinear Schrödinger equation (NSE). This equation, apart from the linear effects of the beam diffraction and frequency dispersion of air, also takes into account the nonlinear polarisability of the medium in an intense optical field. The most significant nonlinear optical effects include the electronic and molecular Kerr effects,

Yu.E. Geints, A.A. Zemlyanov V.E. Zuev Institute of Atmospheric Optics, Siberian Branch, Russian Academy of Sciences, ul. Akad. Zueva, 634021 Tomsk, Russia; e-mail: ygeints@iao.ru

Received 3 August 2009; revision received 2 December 2009
Kvantovaya Elektronika **40** (2) 121 – 126 (2010)
Translated by I.A. Ulitkin

nonlinear refraction and absorption in plasma produced in the beam channel as well as the nonlinearity of highest orders over the field.

In the coordinate system bound with a pulse ($\boldsymbol{r}_\perp, z; t \equiv t' - z/v_{gr}$) moving with the group velocity v_{gr}, the NSE has the form [5, 6]:

$$\left(\frac{\partial}{\partial z} - \frac{\mathrm{i}}{2n_0 k_0 \hat{T}_\partial}\nabla_\perp^2 + \mathrm{i}\frac{k_\omega''}{2}\frac{\partial^2}{\partial t^2}\right)U(\boldsymbol{r}_\perp, z; t)$$

$$- \mathrm{i}k_0\hat{T}_\partial(\tilde{n}_2 - \hat{T}_\partial^{-2}n_\mathrm{p})U(\mathbf{r}_\perp, z; t) + \frac{\alpha_\mathrm{nl}}{2}U(\boldsymbol{r}_\perp, z; t) = 0. \quad (1)$$

Here, $U(\boldsymbol{r}_\perp, z; t)$ is a slowly varying complex electric-field amplitude of the light pulse; $\nabla_\perp^2$ is the transverse Laplacian; n_p is the 'plasma' refractive index of the medium; $k_0 = 2\pi/\lambda_0$ is the wave number; $k_\omega'' = \partial^2 k/\partial\omega^2$ is the dispersion coefficient of the group velocity of the light pulse in the medium; $\tilde{n}_2 = (n_2/2)\int_{-\infty}^{\infty}\mathrm{d}t'\Lambda(t-t')|U(t')|^2$; n_2 is the coefficient taking into account the Kerr nonlinearity of the medium refractive index; $\hat{T}_\partial = 1 + \mathrm{i}\omega_0^{-1}\partial/\partial t$ is the operator taking into account the spatiotemporal focusing ($\hat{T}_\partial^{-1}\nabla_\perp^2$) and self-steepening of the temporal front ($\hat{T}_\partial\tilde{n}_2$) of the radiation pulse; $\Lambda(t)$ is the intertrial polarisability of the medium. Due to the presence of this operator in equation (1), it correctly describes the self-focusing dynamics even for few-cycle optical pulses.

The coefficients of nonlinear absorption α_nl and refraction n_p are coupled with the processes of the medium photoionisation and plasma formation and are represented by the expressions:

$$\alpha_\mathrm{nl} = \sigma_\mathrm{c}\rho_\mathrm{e} + \frac{W(I)}{I}\Delta E_\mathrm{i}(\rho_\mathrm{nt} - \rho_\mathrm{e}), \quad n_\mathrm{p} = \sigma_\mathrm{c}\frac{\tau_\mathrm{ce}\rho_\mathrm{e}}{2n_0},$$

where $W(I)$ is the photoionisation rate (probability) of the molecules in the medium; $I = |U|^2 cn_0/8\pi$ is the radiation intensity; n_0 is the linear refractive index of the medium; ρ_nt is the density of neutral atoms (molecules); σ_c and ΔE_i are the cascade ionisation cross section and ionisation potential of a molecule, respectively; ρ_e is the concentration of free electrons in the beam channel (plasma density) depending on the spatial and temporal coordinates; τ_ce is the characteristic time of collisions of free electrons with heavy particles; $\omega_\mathrm{p} = [e^2\rho_\mathrm{e}/(m_\mathrm{e}\in_0)]^{1/2}$ is the plasma frequency; e and m are the electron charge and mass; ω is the light wave frequency; $\in_0 = 8.8\times10^{-12}$ F m^{-1} is the universal electric constant.

The instantaneous density of free electrons $\rho_\mathrm{e}(\boldsymbol{r}_\perp, z, t)$ in the medium is usually found by using the rate equation, which, on the one hand, yields an increase in the electron density due to the cascade and multiphoton ionisation of molecules and, on the other hand, takes into account the decrease in the electron concentration due to their recombination with ions and neutral atoms. Under condition of the plasma quasi-neutrality and quasi-equilibrium (we deal here with a thermodynamic equilibrium), this equation for the free electron concentration ρ_e has the form:

$$\frac{\partial\rho_\mathrm{e}}{\partial t} = W(I)(\rho_\mathrm{nt} - \rho_\mathrm{e}) + \frac{\sigma_\mathrm{c}}{n_0\Delta E_\mathrm{i}}\rho_\mathrm{e}I - v_r\rho_\mathrm{e}^2 - v_\mathrm{att}\rho_\mathrm{e}, \quad (2)$$

where v_r, v_att are the coefficients of the recombination and attachment rates of the electrons by the neutral molecules, respectively [7].

In the case of the cascade ionisation of atoms, the seed free electrons, which are always present in the medium, acquire the energy in the electromagnetic field of the wave due to the mechanism inverse to the bremsstrahlung and, when colliding with the neutral atoms, can ionise them. The energy of the newly produced electrons during their interaction with a light field also increases, which leads to the appearance of new portion of free charges, etc. Thus, an electron avalanche, during which the concentration of free electrons increases exponentially in time, develops in the medium.

The cascade ionisation cross section in the approximation of the instantaneous energy exchange between an electron and an atom (Drude model) is expressed as follows [7]:

$$\sigma_\mathrm{c} = \frac{\omega_\mathrm{p}^2\tau_\mathrm{ce}}{c\rho_\mathrm{e}(\omega^2\tau_\mathrm{ce}^2 + 1)}. \quad (3)$$

The electron recombination rate, which, in essence, is inverse to the ionisation process, is proportional to the concentration of positive ions and the collision frequency of electrons and ions in the plasma: $v_\mathrm{c} = \tau_\mathrm{ce}^{-1}$. The typical values of v_c in the plasma with the subcritical concentration of electrons are equal to $\sim 10^{13}$ s^{-1} [7] for atmospheric air and $\sim 10^{15}$ s^{-1} [8] for water. In this case, the coefficient of the recombination rate v_r is equal to 2.2×10^{-13} m^3 s^{-1} (O_2) and 2.0×10^{-15} m^3 s^{-1} (H_2O) [8, 9]. For the characteristic time of the electron attachment $\tau_\mathrm{att} = v_\mathrm{att}^{-1}$, there exist the following estimates: $\tau_\mathrm{att} \sim 4\times10^{-8}$ s (O_2) and $\sim10^{-11}$ s (H_2O). One can see that the decrease in the number of free electrons by their attachment to the neutrals is a much slower process compared to the recombination with ions. Therefore, in the further analysis, this channel of the electron concentration decrease will not be taken into account.

Let us discuss the issue of calculating the ionisation rate $W(I)$ of the medium molecules by radiation. According to the classical theory of the multiphoton ionisation [10], an atom can be ionised due to the series absorption of several radiation quanta by this atom during a short interval. The probability of this multiphoton process is proportional to the instantaneous laser radiation intensity to the K power, where K is the integer part of the expression $(\Delta E_\mathrm{i}/\hbar\omega_0 + 1)$ and $\hbar$ is Planck's constant.

Unlike the cascade ionisation, the multiphoton ionisation requires a rather high radiation intensity, but develops significantly faster.

At rather high intensities of radiation affecting the medium (for air, $I \sim 10^{13} - 10^{15}$ W cm^{-2}), one more photoionisation mechanism is possible, namely, tunnel ionisation [10, 11]. The electron in the atom can tunnel through the potential barrier, i.e. become free by absorbing fewer light quanta than in the case of the multiphoton ionisation. In the theory, the boundary between the multiphoton and tunnel ionisation regimes is set by the so-called adiabatic parameter (Keldysh parameter).

To take into account a change in the escape rate of electrons in different photoionisation regimes in the intense light field, there were developed several models; however, one of the most widely used models is the Perelomov–Popov–Terent'ev ionisation theory (PPT theory) [12]. This theory generalises the approach used by Keldysh [10] and takes into account the Coulomb interaction between the ion

residuals and the ionised electron, which reside at any bound energy level of the atom or ion. The specific expressions for calculating the photoionisation rate by the PPT model are presented in many papers (see, for example, reviews [1, 2]); however, below we will use the semiempirical expression $W(I) = A_W(I)I^K$ proposed in [13], where the coefficients A_W and K are calculated in accordance with the medium type and the laser wavelength. This dependence is obtained by approximating the measured ionisation rate of molecular gases by laser radiation [14], is simple to use, and allows one to determine the quantity $W(I)$ with an accuracy sufficient for practical calculations. Thus, according to [13], for atmospheric gases at the laser radiation wavelength $\lambda_0 =$ 800 nm, we obtained the functional dependence of the coefficient A_W:

$$\lg(A_W(I)) = \lg A_0 - A_1 \exp\left[-\frac{\lg^2(I/A_3)}{A_2^2}\right]$$

$$= \lg A_0 - A_1 \exp\left[-\frac{1}{A_2^2}\lg^2\left(\frac{I_0}{I_c}|U|^2\right)\right],$$

where $K = 7.44$, $\lg A_0 = -119.378$ s^{-1} m^{-2K} W^{-K}, $A_1 =$ 13.445, $A_2 = 2.041$, $\lg I_c = 20.616$ W m^{-2} (for O_2) и $K =$ 10.165, $\lg A_0 = -168.530$ s^{-1} m^{-2K} W^{-K}, $A_1 = 19.223$, $A_2 = 2.012$, $\lg A_3 = 20.688$ W m^{-2} (for N_2). We will use below the corresponding expression from paper [10] to calculate the ionisation rates of the water molecules.

It is obvious that the high optical power densities at which the ionisation regime change over can be achieved under real conditions predominantly in gaseous media rather than in the condensed matter. Indeed, in the femtosecond pulse field an optical breakdown [15], which stops self-focusing and blocks the further increase in the laser radiation intensity in the beam channel, develops in water already at $I \sim (2-5) \times 10^{13}$ W cm^{-2}.

The inertial component in the optical Kerr effect is associated with the finite time of anisotropic molecule orientation in the matter along the electric field vector and, in its physical nature, is the Raman self-scattering process of spectral components inside the light pulse spectral width. This inertia of the cubic nonlinear response is usually taken into account in accordance with the damped oscillator model [16] having its own frequency Ω_R and characteristic time τ_d of the oscillation damping. In this case, the full function of the cubic response of the medium to the action of the light field taking into account the instantaneous (electron) and inertial (molecular) polarisability can be represented in the form: $A(t) = (1-\beta)\delta(t) + \beta\theta(t)\Omega_R \times \exp(-t/\tau_d)\sin\Omega_R t$, where $\delta(t)$, $\theta(t)$ are the delta function and Heaviside function, respectively; β is the specific fraction of the inertial part of the Kerr effect. The fitting parameters Ω_R and τ_d in the oscillator model are chosen based on the medium type. The specific fraction β of the Raman effect in the cubic nonlinear polarisation is usually selected at the 0.5 level for atmospheric gases and equal to zero for water.

Table 1 lists the most frequently used values of the parameters of the ultrashort pulse self-focusing and filamentation model (1), (2) for air and water. The analysis of the presented data allows a conclusion about the peculiarities of the light pulse self-focusing in the media under study.

One can see that compared to air, the femtosecond pulse self-action in water is characterised by a significantly lower parameter of the critical self-focusing power $P_{cr} = \lambda_0/(n_0 k_0 n_2)$. This is caused by the corresponding difference in the values of the nonlinear coefficient n_2 in water and air. In addition, the significant difference in the chromatic dispersion coefficients k''_ω in the media under study also draws our attention. This circumstance proves to be very important in studying the radiation self-focusing in media with a strong dispersion, because the account for it increases the effective critical power P_{cr} with increasing the laser pulse duration [17, 21].

In studying the ultrashort pulse filamentation, it is important to know the characteristics of the filaments being produced: characteristic intensity of the optical field in the filament, its radius, concentration of free electrons in the plasma. We will consider these parameters in water and air by using the numerical simulation of radiation propagation in these media.

3. Discussion of the numerical results of filamentation simulation

The calculations were performed by using equations (1), (2) and the values of the optical parameters of each of the medium (see Table 1). The initial laser beam was set in the form of a weakly focused radiation with a Gaussian envelope over the spatial and time coordinates:

$$U(\boldsymbol{r}_\perp, z=0, t) = U_0 \exp[-|\boldsymbol{r}_\perp|^2/(2R_0)^2 - t^2/(2t_p)^2]$$

$$\times \exp(-ik_0 n_0 |\boldsymbol{r}_\perp|^2/F).$$

We considered pulsed radiation from a Ti : sapphire laser with the central wavelength $\lambda_0 = 800$ nm, pulse duration (at the e^{-1} level) $t_p = 100$ fs, and the initial beam radius $R_0 = 1$ mm. The initial radius of the phase front curvature F was selected for definiteness equal to $0.1L_R$, where $L_R = \frac{1}{2}(n_0 k_0 R_0^2)$ is the Rayleigh beam length. The initial peak power P_0 in the radiation pulse corresponded to the ten-fold excess over the critical self-focusing power: $P_0 = 10P_{cr}$, i.e., was 32 GW and 38 MW for air and water, respectively.

Figure 1 shows the evolution of the laser beam radius along its propagation path. The beam is characterised by the geometrical radius R_1 determined by the beam energy density profile $w(\boldsymbol{r}_\perp, z) = \int_{-\infty}^{\infty} I(\boldsymbol{r}_\perp, z; t')dt'$ at the 1/e level with respect to its maximum, and the effective radius R_{eff},

Table 1. Values of the parameters of the ultrashort pulse filamentation model for atmospheric gases and water ($\lambda = 800$ nm).

Medium	n_0	n_2/ m^2 W^{-1}	k''_ω/ s^2 m^{-1}	P_{cr}/W	ΔE_i/eV	τ_{ce}/s	K	$\nu^{(K)}$/W$^{(1-K)}$ ×m$^{(2K-3)}$	σ_c/m^2	ν_r/m^3 s^{-1}	ρ_{nt}/m^3	Ω_R/Hz	τ_d/s	β	P_c/W
Gas	1.0	3.2×10^{-23} [17, 18]	2.1×10^{-29} [19]	3.18×10^9	12.1 (O_2) 15.6 (N_2)	3.5×10^{-13} [7, 8]	8 (O_2) 11 (N_2)	7.8×10^{-123} (O_2) 6.04×10^{-179} (N_2)	5.52×10^{-24}	1.1×10^{12} [8, 20]	5.0×10^{24} (O_2) 2.1×10^{25} (N_2)	2.0×10^{13} [16]	7.7×10^{-14} [16]	0.5 [16]	3.2×10^9
Water	1.33	2.0×10^{-20} [17, 18]	3.0×10^{-27} [19]	6.5×10^6	6.5	3.0×10^{-15} [7, 8]	5	2.5×10^{-63}	6.29×10^{-22}	2.05×10^{-15} [8, 20]	3.3×10^{28}	–	–	0 [16]	3.8×10^6

which is calculated as the time-integrated normalised second-order moment of the light wave intensity:

$$R_{\text{eff}}(z) = \left[\frac{1}{W(z)}\int_{-\infty}^{\infty} \mathrm{d}t' \iint_{\boldsymbol{R}_\perp} \mathrm{d}^2\boldsymbol{r}_\perp I(\boldsymbol{r}_\perp, z; t') \times |(\boldsymbol{r}_\perp - \boldsymbol{r}_{\text{gr}})|^2\right]^{1/2},$$

where r_{gr} is the radius vector of the centre of gravity of the beam intensity distribution over its cross section; W is the total energy in the radiation pulse; $\boldsymbol{R}_\perp$ is the spatial integration region. The parameter R_{eff} turns useful in analysing the beam intensity profiles because, according to the definition, the effective radius determines the dimension of the spatial region in which no less than 50 % of the total light beam energy is concentrated. For the Gaussian transverse profile, the intensities R_1 and R_{eff} have one and the same value.

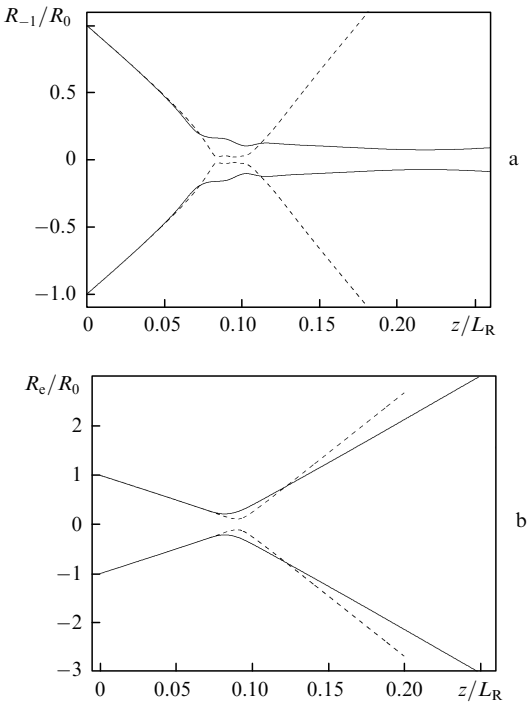

Figure 1. Dependences of the relative geometrical (a) and effective (b) laser beam radii during the filamentation in air (solid curve) and in water (dashed curves) on the normalised distance.

One can see from Fig. 1 that the initial stages of the beam radius evolution in air and water proceed similarly, the beam being compressed in a self-induced manner and its geometrical radius R_1 decreasing in the filamentation region down to $R_{\text{eff}} \sim 10$ and 70 μm, respectively. However, in air the filament is produced somewhat closer to the path beginning and is substantially longer over z compared to that in water. The additional calculations of the filamentation dynamics, we performed for a longer path (not presented here), show that for the given radiation parameters the filament length in air is comparable with the Rayleigh beam length, i.e., is of the order of several meters. In water, as one can see from Fig. 1a, the length of the extremely high radiation localisation region was only equal to 15 cm.

The evolutional dependence of the effective beam radius R_{eff} during its self-focusing, unlike the spatial dynamics of the central part, i.e., the region, in which a light filament is produced, has a pronounced focal waist. This waist, as is seen from Fig. 1, is located in the filamentation region and corresponds to the position of the so-called global nonlinear focus of the beam [13]. In water, the global nonlinear focus is located more to the right on the evolutional variable than in air and virtually coincides with the geometrical focus of the beam. After propagating through the global nonlinear focus, the effective beam radius starts increasing stably, the beam acquiring the effective nonlinear angular divergence $\theta_{\text{eff nl}} = \lim_{z\to\infty} (\frac{1}{2}\mathrm{d}^2 R_{\text{eff}}^2/\mathrm{d}z^2)^{1/2}$, which both in air and water exceeds the initial beam divergence θ_0. Besides, in water $\theta_{\text{eff nl}}$ is 1.5 times higher than in air ($\theta_{\text{eff nl}}/\theta_0 = 2.27$ versus 1.5).

Note that the appearance of the additional nonlinear beam divergence during the its filamentation is caused by the accumulation of the amplitude–phase distortions of the initial light wave profile due to its self-modulation in the Kerr medium as well as due to the multiphoton absorption and the plasma nonlinearity.

Figure 2 presents the maximum values of the free electron densities $\rho_{\text{e max}}$ and radiation intensity $I_{\max}$ realised in the beam channel during the action of the laser pulse at different points of the path. One can see that in the region of the filament existence the values of these parameters weakly change with distance. In this case, the characteristic intensity in the filament in air is an order of magnitude higher than in water: $I_{\text{f}} \sim 30 - 40$ TW cm^{-2}. The maximum plasma density in the filament produced in air is, on the contrary, smaller than the free electron density in the filament produced in water (Fig. 2a).

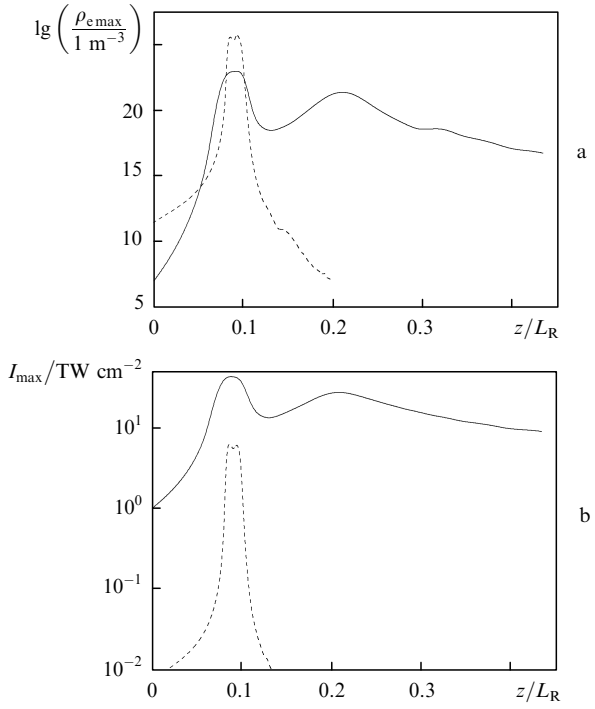

Figure 2. Dependences of the maximum density of the free electrons in the beam channel (a) and the maximum laser pulse intensity (b) on the normalised longitudinal distance for air (solid curves) and water (dashed curves).

It follows that the cascade mechanism of the medium ionisation plays an important role in the development of the plasma bunch. In the condensed medium, the cross section of the cascade ionisation process is two orders of magnitude larger than in the gas (see Table 1). Due to this, in air, unlike water, this mechanism gets actively into the action already at the electron densities $\sim 10^{20}$ m^{-3}, i.e., the ionisation of the atoms during their collision with free charges begins to dominate over the direct photoionisation, thereby favouring the exponential rise in the electron density even in the case of an insignificant increase in the light wave intensity in the filament region.

The characteristic values of the radiation intensity I_f, the free electron density ρ_f in the filament, as well as its radius R_f achieved in air and water for the given parameters of the laser pulse are shown in Table 2.

Table 2. Characteristic parameters of the filamentation region.

Medium	I_f/TW cm^{-2}	R_f/μm	ρ_f/m^{-3}
Air	44 – 65	30 – 40	$2 \times 10^{21} - 6 \times 10^{22}$
Water	6 – 7	5 – 10	$(3 - 5) \times 10^{25}$

Consider one more characteristic of laser radiation which is fundamentally important for femtosecond optics, namely, the spectral composition of radiation experiencing filamentation on the path. The spectral power density of the laser pulse

$$P(z, \lambda) = \iint_{\boldsymbol{R}_\perp} \mathrm{d}^2 \boldsymbol{r}_\perp |\tilde{S}(\boldsymbol{r}_\perp, z; \lambda)|^2$$

($\tilde{S}$ is the Fourier transform of the temporal field envelope) after propagating some distance in air and in water is shown in Fig. 3.

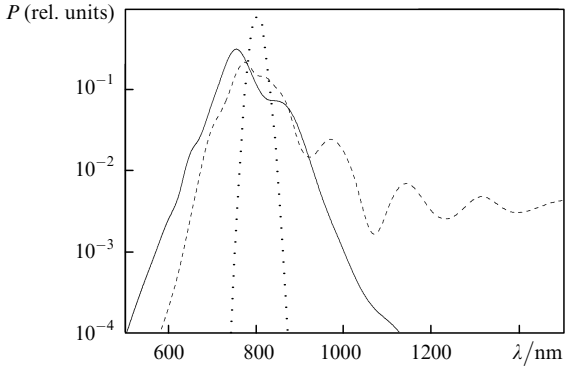

Figure 3. Laser pulse spectra at the point $z = 0.4L_R$ during the filamentation in air (solid curve) and in water (dashed curve). The dotted curve shows the initial laser radiation spectrum.

The presented spectra have the features of the self-phase modulation of the ultrashort pulses, which proceeds in the presence of the strong Kerr and plasma nonlinearities. One can see the spectrum broadening, the shift of its maximum to the red, the formation of the supercontinuum wings in the blue and red spectra.

Unlike air, where the spectral broadening is more or less symmetric on the both sides of the spectrum, in water the filamentation leads to the formation of an extended wing in the long-wave region. This is caused by the action of the inertial part of the Kerr nonlinearity (stimulated Raman scattering), which is manifested stronger in water than in a gaseous medium. On the whole, the effective (root-mean-square) spectral widths [22] are by ~ 15 % larger in the case of water.

This fact is explained within the framework of the classical model of the one-dimensional propagation of the light wave in an optically nonlinear medium [23]. The frequency change of this wave, $\delta\omega = \omega - \omega_0$, at a distance z due to the self-modulation is determined by the nonlinear component of the wave phase φ_{nl} as follows: $\delta\omega(z, t) = -\partial\varphi_{nl}(z, t)/\partial t$. By using expressions (1) – (3), we obtain

$$\delta\omega(\boldsymbol{r}_\perp, z, t) = -k_0 z \frac{\partial(\delta n)}{\partial t}$$

$$\approx k_0 z \left[-\frac{n_2}{n_0}\frac{\partial I}{\partial t} + \frac{\nu^{(K)}}{2n_0\rho_c\Delta E_i} I^K \exp\left(\nu_{cas} \int_{-\infty}^{\infty} I \mathrm{d}t \right) \right], \quad (4)$$

where

$$\nu^{(K)} = \rho_{nt} W \Delta E_i I^{-K}; \quad (5)$$

ν_{cas} is the coefficient of the cascade ionisation rate. It follows from this expression that the self-phase modulation of the pulse leads to its spectral broadening proportional, first of all, to the light wave intensity. Because the beam filamentation region is characterised by the highest intensity, the main spectrum transformation of the pulse occurs in this region. Therefore, to increase the spectral width Δ_ω of radiation average over the light beam cross section on the filamentation path, we can write approximately:

$$\Delta_\omega(z) = \frac{\iint_{\boldsymbol{R}_\perp} \delta\omega(\boldsymbol{r}_\perp, z, t) \mathrm{d}\boldsymbol{r}_\perp}{\iint_{\boldsymbol{R}_\perp} \mathrm{d}\boldsymbol{r}_\perp} \approx k_0 l_f \frac{R_f^2}{R_0^2} G(I_f),$$

where l_f is the filament characteristic length and $G(I_f)$ is the coefficient specified by the expression in square brackets in the right-hand side of (4), whose quantity is determined by the parameters of the medium optical nonlinearity. At the identical initial relative power of the laser pulse in water, the filament is approximately an order of magnitude shorter than in air, and in addition, two orders of magnitude thinner in the transverse cross section (see Fig. 1a and Table 2). In this case, it is easy to see that in water the coefficient G is almost three orders of magnitude higher due to the large constants of nonlinear interactions. As a result, the total spectral broadening of the pulse in both media under study has the same order. The numerical calculation yields $\Delta_\omega(L)/\Delta_\omega(0) = 6.2$ (air) and 7.3 (water) for this parameter.

4. Conclusions

Therefore, we have considered the filamentation properties of the ultrashort pulses with the carrier wavelength $\lambda_0 = 800$ nm in two natural media – water and air. Within the framework of the universal scenario of the nonstationary radiation self-focusing, we have performed a qualitative and quantitative comparative analysis of the basic parameters of the beam filamentation region and the transformation degree of its characteristics. The analysis has shown that the drastic differences in the optical parameters of water and air, and, first of all, in the

coefficients of the Kerr nonlinearity and the ionisation of the medium molecules, lead to changes in the key characteristics producing light and plasma filaments in the beam channel.

It follows from the calculations that when selecting the initial laser pulse power with the identical excess of the critical self-focusing power in each of the media under study, the filaments appearing in water are 4–6 times thinner on average than in air. The average radius of the light filament in water does not exceed 10 μm and its length is almost an order of magnitude smaller than in air. The characteristic radiation intensity in the filament produced in air is ~ 50 TW cm^{-2}, which is an order of magnitude greater than the intensity in the filament appearing in water. However, the peak density of the free electrons in the plasma channel of the filament in air is two orders of magnitude smaller than in water and lies in the region $10^{21} - 10^{23}$ m^{-3}.

The average angular divergence of laser radiation propagated through the filamentation region, which is determined by the evolutional dependence of the effective radius of the light pulse in water, proves to be almost twice higher than in air, which results in a higher increase in the effective transverse area of the beam after the global nonlinear focus. In this case, the average width of the supercontinuum spectrum produced during the beam filamentation has close values both in air and water, which is caused by its complex dependence on the filament length and on the 'force' of the optical nonlinearity of the medium.

Acknowledgements. This work was supported by the Integration Project of the Siberian Branch.

References

1. Bergé L., Skupin S., Nuter R., Kasparian J., Wolf J.-P. *Rep. Prog. Phys.*, **70**, 1633 (2007).
2. Couairon A., Mysyrowicz A. *Phys. Reports*, **441**, 47 (2007).
3. Kasparian J., Wolf J.-P. *Opt. Express*, **16**, 466 (2008).
4. Kandidov V.P., Shlenov S.A., Kosareva O.G. *Kvantovaya Electron.*, **39**, 205 (2009) [*Quantum Electron.*, **39**, 205 (2009)].
5. Brabec T., Krausz F. *Phys. Rev. Lett.*, **78**, 3282 (1997).
6. Porras M.A. *Phys. Rev. A*, **60**, 5069 (1999).
7. Raizer Yu.P. *Gas Discharge Physics* (Berlin: Springer-Verlag, 1991; Moscow: Nauka, 1987).
8. Schwarz J., Diels J.-C. *Phys. Rev. A*, **65**, 013806 (2001).
9. Tzortzakis S., Prade B., Franco M., Mysyrowicz A. *Opt. Commun.*, **181**, 123 (2000).
10. Keldysh L.V. *Zh. Eksp. Teor. Fiz.*, **47**, 1945 (1964).
11. Delone N.B., Krainov V.P. *Nelineinaya ionizatsiya atomov lazernym izlucheniem* (Nonlinear Ionisation of Atoms by Laser Radiation) (Moscow: Fizmatlit, 2001).
12. Perelomov A.M., Popov V.S., Terent'ev M.V. *Zh. Eksp. Teor. Fiz.*, **50**, 1393 (1966).
13. Geints Yu.E., Zemlyanov A.A. *Opt. Atmos. Okean.*, **21**, 793 (2008).
14. Talebpour A., Yang J., Chin S.L. *Opt. Commun.*, **163**, 29 (1999).
15. Vogel A., Noack J., Nahen K., Theisen D., Busch S., Parlitz U., Hammer D.X., Noojin G.D., Rockwell B.A., Birngruber R. *Appl. Phys. B*, **68**, 271 (1999).
16. Sprangle P., Penano J.R., Hafizi B. *Phys. Rev. E*, **66**, 046418 (2002).
17. Nibbering E.T.J., Franco M.A., Prade B.S., Grillon G., Le Blanc C., Mysyrowicz A. *Opt. Commun.*, **119**, 479 (1995).
18. Ripoche J.F., Grillon G., Prade B.S., Franco M.A., Nibbering E.T.J., Lange H.R., Mysyrowicz A. *Opt. Commun.*, **135**, 310 (1997).
19. Liu W., Kosareva O.G., Golubtsov I.S., Iwasaki A., Becker A., Kandidov V.P., Chin S.L. *Appl. Phys. B*, **76**, 215 (2003).
20. Fan C.H., Sun J., Longtin J.P. *J. Appl. Phys.*, **91**, 2530 (2002).
21. Luther G.G., Moloney J.V., Newell A.C., Wright E.M. *Opt. Lett.*, **19**, 862 (1994).
22. Geints Yu.E., Zemlyanov A.A. *Opt. Atmos. Okean.*, **18**, 574 (2005).
23. Akhmanov S.A., Vysloukh V.A., Chirkin A.S. *Optics of Femtosecond Laser Pulses* (New York: American Institute of Physics, 1992; Moscow: Nauka, 1988).